# Identification and functional characterization of the Arabidopsis Snf1-related protein kinase SnRK2.4 phosphatidic acid-binding domain

Julkowska, M.M.; McLoughlin, F.; Galvan-Ampudia, C.S.; Rankenberg, J.M.; Kawa, D.; Klimecka, M.; Haring, M.A.; Munnik, T.; Kooijman, E.E.; Testerink, C.

**DOI**
10.1111/pce.12421

**Publication date**
2015

**Document Version**
Final published version

**Published in**
Plant, cell and environment

**License**
CC BY-NC-ND

Plant, Cell & Environment

*Plant, Cell and Environment* (2015) **38**, 614–624 doi: 10.1111/pce.12421

## Original Article

# Identification and functional characterization of the *Arabidopsis* Snf1-related protein kinase SnRK2.4 phosphatidic acid-binding domain

Magdalena M. Julkowska[1]*, Fionn McLoughlin[1]*, Carlos S. Galvan-Ampudia[1], Johanna M. Rankenberg[1,2,3], Dorota Kawa[1], Maria Klimecka[4], Michel A. Haring[1], Teun Munnik[1], Edgar E. Kooijman[2,3] & Christa Testerink[1,3]

[1]*Plant Physiology, Swammerdam Institute for Life Sciences, University of Amsterdam, 1098 XH Amsterdam, The Netherlands,* [2]*Department of Biological Sciences, Kent State University, Kent, OH 44242, USA,* [4]*Institute of Biochemistry and Biophysics, Polish Academy of Sciences, 02-106 Warsaw, Poland and* [3]*International Institute for Complex Adaptive Matter, University of California, Davis, CA 95616 USA*

## ABSTRACT

**Phosphatidic acid (PA) is an important signalling lipid involved in various stress-induced signalling cascades. Two SnRK2 protein kinases (SnRK2.4 and SnRK2.10), previously identified as PA-binding proteins, are shown here to prefer binding to PA over other anionic phospholipids and to associate with cellular membranes in response to salt stress in *Arabidopsis* roots. A 42 amino acid sequence was identified as the primary PA-binding domain (PABD) of SnRK2.4. Unlike the full-length SnRK2.4, neither the PABD-YFP fusion protein nor the SnRK2.10 re-localized into punctate structures upon salt stress treatment, showing that additional domains of the SnRK2.4 protein are required for its re-localization during salt stress. Within the PABD, five basic amino acids, conserved in class 1 SnRK2s, were found to be necessary for PA binding. Remarkably, plants overexpressing the PABD, but not a non-PA-binding mutant version, showed a severe reduction in root growth. Together, this study biochemically characterizes the PA–SnRK2.4 interaction and shows that functionality of the SnRK2.4 PABD affects root development.**

*Key-words*: phosphatidic acid; phospholipid binding; root system architecture; SnRK2.10

## INTRODUCTION

Environmental stress causes changes in the phospholipid composition of cellular membranes. Several low abundant phospholipids, including phosphoinositides (PPIs) and phosphatidic acid (PA) that act as lipid second messengers, are involved in a wide array of cellular responses (Meijer & Munnik 2003; Wang 2004; Arisz *et al*. 2009; Xue *et al*. 2009). PA is involved in stress responses as well as in development and metabolic processes (Testerink & Munnik 2011). It is normally present in small amounts, but rapidly accumulates in the lipid bilayer in response to different biotic and abiotic stress stimuli, including drought and salinity. PA is predominantly produced through two different pathways. Phospholipase D (PLD) hydrolyses structural phospholipids into PA and a remaining head group (Wang 2004; Bargmann & Munnik 2006) and phospholipase C (PLC) hydrolyses PPIs to produce diacylglycerol (DAG) (Munnik & Vermeer 2010). DAG is subsequently phosphorylated to PA by DAG kinase (DGK). Osmotic stress induces an increase in PA through both pathways (Arisz *et al*. 2009).

Several PLDs have been implicated in salt stress acclimation in *Arabidopsis*. A *pldα3* knockout (KO) mutant was shown to exhibit reduced primary root growth and a reduction in the number of lateral roots in hyperosmotic conditions (Hong *et al*. 2008). A similar observation was made in a *pldα-1/δ* double mutant, which displayed lower PA accumulation in response to salt and its seedlings showed reduced primary root growth in saline conditions (Bargmann *et al*. 2009). For stress-induced PA formation via DGK activity, no genetic evidence has been found so far, probably due to genetic redundancy (Arisz *et al*. 2013). Chemical inhibitor studies and differential labelling studies did reveal a role for DGK activity in cold-induced PA responses (Gomez-Merino *et al*. 2005; Arisz *et al*. 2013). Moreover, treatment with a DGK inhibitor was found to affect the expression of the drought-induced DREB transcription factors, through an unknown mechanism (Djafi *et al*. 2013).

Recently, PA has been identified as an important factor in the maintenance of root growth in adverse conditions through binding of an array of proteins that are directly involved in the regulation of the root system architecture (as reviewed in McLoughlin & Testerink 2013; Pierik

*Correspondence: C. Testerink. e-mail: c.s.testerink@uva.nl*

*These authors contributed equally to this work.

& Testerink 2014). In an affinity proteomics screen for PA-binding proteins (Testerink *et al*. 2004), a number of proteins involved in metabolism and stress signalling were identified, including the Arabidopsis Sucrose-non-fermenting 1 Related protein Kinases 2.4 (SnRK2.4/SRK2A) and 2.10 (SnRK2.10/SRK2B). Both protein kinases belong to the plant-specific SnRK2 class (SnRK2) (Kobayashi *et al*. 2004; Umezawa *et al*. 2004; Kulik *et al*. 2011), which are activated in response to salt and osmotic stress (Munnik *et al*. 1999; Mikolajczyk *et al*. 2000; Boudsocq *et al*. 2004; McLoughlin *et al*. 2012). Based upon phylogeny, the SnRK2 family has been divided into three classes (Kobayashi *et al*. 2004), which differ in their activation by the phytohormone abscisic acid (ABA). In *Arabidopsis*, SnRK2.2 (SRK2D), 2.3 (SRK2I) and 2.6 (OST1; SRK2E) are strongly activated in the presence of ABA (class 3). Together with the components PYR1, ABI1 and ABF2, the SnRK2.6/2.2/2.3 protein kinases were shown to be sufficient for ABA-induced-gene expression, and to act in the core ABA signalling pathway (Fujii *et al*. 2009). SnRK 2.7 and 2.8 (class 2) are involved in drought signalling (Umezawa *et al*. 2004; Mizoguchi *et al*. 2010). The members of SnRK2 class 1, SnRK2.1 (SRK2G), SnRK2.4 (SRK2.4A), SnRK2.5 (SRK2H) and SnRK2.10 (SRK2B) are activated by osmotic stress, but not by ABA (Boudsocq *et al*. 2004; Umezawa *et al*. 2004; Boudsocq & Lauriere 2005). SnRK2.4 and 2.10 are among the most rapidly activated protein kinases in response to salt and are involved in the maintenance of root system architecture under saline conditions (McLoughlin *et al*. 2012). SnRK2.4 was recently shown to bind PA *in vitro*, and SnRK2.4-YFP accumulates in punctate structures in response to salt (McLoughlin *et al*. 2012), suggesting a role for membrane association in the response to salt stress.

In this study, the significance of SnRK2.4's interaction with PA was examined. We show that SnRK2.4 targeted to punctate structures is directly associated with cellular membranes *in vivo*. The PA-binding domain (PABD), overlapping with the abiotic stress domain 1 (Kulik *et al*. 2011), was found to be sufficient for PA binding *in vitro*. However, the same domain fused to YFP, or SnRK2.4's close homolog SnRK2.10, failed to localize to punctate structures *in planta*, showing that PA binding is not sufficient for accumulation in these punctate structures. Replacing several conserved basic amino acids in the PABD with alanines resulted in loss of binding. Moreover, overexpression of the PABD *in planta* reduced root growth only when these conserved amino acids were unaltered, suggesting that the PABD identified in domain 1 contributes to SnRK2.4 functional regulation and can interfere with root growth, possibly by competing for PA binding with other regulators.

## MATERIALS AND METHODS

### Cloning and site-directed mutagenesis

SnRK2.4, 2.10 and 2.6 FL CDS, fragments A–F, SnRK2.6 kinase domain, PABD, PABD$^{R266A,\ K278A,\ K279A,\ K294A,\ K300A}$, SnRK2.4$^{R266A,\ K278A,\ K279A,\ K294A,\ K300A}$ and SnRK2.4$^{K27A,\ K222A,\ R266A,\ K278A,\ K279A,\ K294A,\ K300A}$ were amplified excluding the terminator with primers containing the gateway recombination attB1 and attB2 site sequences (Supporting Information Table S1), which are compatible with the recombination sites of pDONR207. The fragments were recombined in pDONR207 using BP2 Clonase according to the instructions of the manufacturer (Invitrogen, Breda, the Netherlands), resulting in pENTR(x) constructs, which were all verified by sequencing. Subsequently, all constructs were recombined into a pGEX-KG gateway expression vector (Dhonukshe *et al*. 2010) using LR Clonase, according to the instructions of the manufacturer (Invitrogen). The constructs were transformed to *Escherichia coli* strain BL21 DE3 for protein expression and purification. The pENTR-PABD was recombined into the expression clone pGII0125-R4R3 (Galinha *et al*. 2007) using three-way gateway, together with the ubiquitin 10 promoter, which was amplified by genomic Col-0 DNA (1986 bp upstream from the start codon) with primers containing appropriated attB recombination sites (Table S1) (Galvan-Ampudia *et al*., unpublished results) (box 1) and mVenus (box 3) (Nagai *et al*. 2002) using LR+ Clonase according to the instructions of the manufacturer (Invitrogen) (pGII0125-R4R3 Norf/pGEM, box 1: promUBQ10/pDONR207; box 2: PCR product PABD/pGEM; box 3: mVENUS FLAG t35). Constructs were transformed using the *Agrobacterium tumefaciens* strain GV3103 to Col-0 through floral dip transformation (Clough & Bent 1998). Several primary transformants were selected using 0.3 $\mu$g mL$^{-1}$ norflurazon, and the plants were allowed to self-pollinate.

Mutations were induced through site-directed mutagenesis with the indicated primers (Table S1). Mutations were sequentially applied in the pENTRY-SnRK2.4 and pENTRY-PABD clones. Mutations were introduced using *Pfu* polymerase (Promega, Leiden, the Netherlands) according to the manufacturer's instructions. The PCR was conducted in a volume of 50 $\mu$L using 10 ng plasmid as template, applying 21 cycles, annealing temperature: 52 °C and an extension time of 16 min. The PCR product was digested with DPNI (Fermentas St. Leon-Rot, Germany) at 37 °C for 2 h and the digestion product was purified using the GeneJet PCR purification kit (Fermentas) according to the manufacturer's instructions and eluted in 30 $\mu$L MQ. The product was transformed into *E. coli* strain DH5$\alpha$. Plasmids were isolated and sequenced to determine if they contained the desired mutation.

### Induction and purification of GST-tagged SnRK2.4 protein fragments from *E. coli*

Transformed BL21 DE3 bacteria were grown overnight at 37 °C in 2xYT medium containing ampicillin. Four millilitres of o/n culture was diluted in 100 mL of pre-warmed 2xYT medium and was grown at 37 °C until $OD_{600}$ reached 0.6. The production of recombinant protein was induced by addition of IPTG up to 1 mM final concentration. The cells were induced for 6 h at 18 °C. Subsequently, cells were centrifuged at 5000 *g* for 15 min at 4 °C. The pellet was snap-frozen in liquid nitrogen and subsequently dissolved in PBS containing 1x complete protease inhibitor cocktail (Boehringer

Ingelheim, Alkmaar, the Netherlands). Cell contents were released by lysozyme treatment and sonication. Soluble proteins were isolated by spinning the cell suspension at 13 500 *g* for 30 min at 4 °C. The SnRK2.4 fragments were purified from soluble protein fraction using the GST-Sepharose beads. Proteins bound to the GST-Sepharose beads were eluted using elution buffer containing 20 mM reduced glutathione (50 mM Tris, pH 8.0). The protein concentration was determined by separating the proteins on sodium dodecyl sulphate–polyacrylamide gel electrophoresis (SDS-PAGE), staining of the gel with colloidal Coomassie (Sigma-Aldrich, Zwijndrecht, the Netherlands) and comparison to known bovine serum albumin (BSA) dilution series.

## Liposome binding assays

Liposome assays were performed as described in Julkowska *et al*. (2013), with some modifications. Per sample, 400 nmol of total lipids was used, unless indicated otherwise. Synthetic 1,2-dioleoyl-sn-glycero-3-phosphatidylcholine (DOPC), 1,2-dioleoyl-sn-glycero-3-phosphatidyletanolamine (DOPE), 1,2-dioleoyl-sn-glycero-3-phosphatidylserine (DOPS), 1,2-dioleoyl-sn-glycero-3-phosphate (DOPA) dissolved in chloroform, natural L-$\alpha$-phosphatidylinositol-4-phosphate (PIP) and L-$\alpha$-phosphatidylinositol-4,5-bisphosphate ($PIP_2$) (brain, porcine-triammonium salt) in chloroform:methanol:water (20:9:1) were used (all from Avanti Polar Lipids, Alabaster, AL, USA). Liposomes were added to 500 ng purified GST-tagged protein and incubated for 30–45 min. Liposomes were harvested by centrifugation at 16 000 *g* for 30 min, washed once in binding buffer and re-suspended in sample buffer. Samples were incubated at 95 °C for 5 min and run on 10% SDS-PAGE, blotted on Hybond-ECL and GST-tagged proteins were detected through Western blot analysis. $IgG_1$ αGST mouse monoclonal (Santa Cruz, Heidelberg, Germany) was used as the primary antibody and goat anti-mouse-HRP (horseradish peroxidase) (Sigma-Aldrich) as the secondary antibody according to the manufacturer's instructions.

## Fractionation

Col-0 plants were grown in hydroponics, similar to the in-gel kinase assay (McLoughlin *et al*. 2012). Further, 40 mL of root material was harvested of salt-stressed roots (150 mM NaCl, 7 min, approximately 200 plants per sample). Fractionation was essentially performed as described in previous works (Monreal *et al*. 2010; McLoughlin *et al*. 2012, 2013), with some modifications. The peripheral membranes were eluted by thoroughly homogenizing the pellet in protein extraction buffer supplemented with 100 mM $Na_2CO_3$. After homogenizing, samples were incubated for 15 min on ice and the sample was spun again at 50 000 *g* for 1 h. The supernatant is shown as the peripheral membrane proteins and the pellet is the remaining pellet. The antibodies raised against specific protein markers were obtained from Agrisera, Vännäs, Sweden, unless stated otherwise: PM ATPase (Palmgren *et al*. 1991), PerM V-ATPase (At4g11150), ER/EndoM SAR1 (At3g62560), Cyt. UGPase (raised against barley) and SnRK2.4/2.10 (Vlad *et al*. 2010). Silver staining was conducted as a loading control. Protein abundances were quantified using ImageJ (NIH, Bethesda, MD, USA).

## Confocal microscopy of SnRK2.4-YFP, PABD-YFP, SnRK2.4-GFP and SnRK2.10-GFP lines

The green fluorescent protein (GFP) fluorophore was excited with argon 488 nm, emission was detected between 505 and 555 nm. The YFP fluorophore was excited with argon 514 nm and emission was detected between 525 and 555 nm. Pictures were taken with a Nikon A1 (Nikon Instruments Europe, BV, Amsterdam, The Netherlands) with a 20× water lens and processed using ImageJ.

## Root system architecture assay

Seeds were surface-sterilized in a desiccator of 1.6 L volume using 20 mL household bleach and 600 $\mu$L 40% HCl for 3 h. The seeds were stratified in 0.1% agar at 4 °C for 48 h and sown on square Petri dishes containing ½ Murashi–Skoog, 0.5% sucrose, 0.1% monohydrate-morpholine-4-ethanesulfonic acid hydrate (MES), monohydrate and 1% daishin agar, pH 5.8 (KOH). Seeds were germinated under long day conditions (21 °C, 70% humidity, 16/8 h light/dark cycle). Four-day-old seedlings were transferred to new agar plates for root system architecture phenotyping. Plates were scanned with an Epson Perfection V700 Scanner (Epson Europe B.V., Amsterdam, The Netherlands) at 200 dpi at 4 d after transfer. Root system architecture was quantified using EZ-Rhizo software (Armengaud 2009). Further, $n = 18$ per line per treatment. Two independent transformants per transgenic line were tested, and two independent biological replicates were performed.

## Identification of fusion proteins with YFP/mCherry

Ten-day-old seedlings of Col-0, UBQ::PABD-YFP, UBQ:: non-PABD-mCherry and 35S::YFP grown as described for the root system architecture assay were used for protein extraction. Protein extracts were prepared by incubating the ground tissue at 4 °C with 3 volumes of extraction buffer [150 mM NaCl, 1% NP-40, 50 mM Tris–HCl (pH 8.0), 1 mM ethylenediaminetetraacetic acid (EDTA), 10 mM NaF, 25 mM $\beta$-glycerophosphate, 1x complete protease inhibitor cocktail (Roche, Boehringer, Amere, The Netherlands)] followed by 20 min of centrifugation at 26 000 *g* (4 °C). Protein concentration was determined using bicinchoninic acid protein assay kit (Sigma-Aldrich). Samples were incubated at 95 °C for 5 min with sample buffer ran on 10% SDS-PAGE, blotted on Hybond-ECL and tagged proteins were detected through Western blot analysis. IgG $\alpha$-GFP rabbit polyclonal (Invitrogen, Eugene, OR, USA) and $\alpha$-mCherry goat polyclonal (Sicgen, Carcavelos, Portugal) were used as the primary

antibody and goat anti-rabbit and rabbit anti-goat-HRP respectively (Pierce, Breda, the Netherlands) as the secondary antibodies according to the manufacturer's instructions. Two independent transformant lines per construct were tested (Supporting Information Fig. S4). Col-0 and 35S::YFP lines were used as negative and positive controls, respectively.

## RESULTS

### SnRK2.4 and 2.10 specifically bind to liposomes containing PA

The protein kinase SnRK2.10 was identified to bind PA *in vitro* in a PA-binding affinity screen using PA-coated Sepharose beads followed by identification through mass spectrometry (Testerink *et al*. 2004). Subsequently, both SnRK2.10 and 2.4 were shown to bind PA directly (McLoughlin *et al*. 2012). To further characterize their lipid binding affinity and specificity, liposome-binding assays were performed with different phospholipid compositions (Fig. 1a). The structural phospholipids PC and PE were used as the basic lipid composition of the liposomes, in which different anionic and signalling lipids were mixed. Purified *E. coli*-expressed GST-fused SnRK2.4 and SnRK2.10 were tested for binding to liposomes containing PA or other negatively charged phospholipids; phosphatidylserine (PS), phosphatidylinositol-4-phosphate (PI4P) and phosphatidylinositol-4,5-biphosphate ($PIP_2$) as controls. The liposomes were composed of 50% structural lipids and 50% of anionic phospholipids to determine *in vitro* PA binding. Both SnRK2.4 and 2.10 showed similar lipid binding properties and specifically bound to liposomes containing PA, but not to liposomes containing other anionic (PS) or anionic phosphorylated lipids (PI4P and $PIP_2$).

### SnRK2.4/2.10 associate with membranes and are present in endomembrane compartments in *Arabidopsis* root tissue in saline conditions

SnRK2.4/2.10 were shown to re-localize to the microsomal membrane fraction in *Arabidopsis* roots (McLoughlin *et al*. 2012). To further investigate which subcellular fraction SnRK2.4/2.10 localize upon salt treatment, *Arabidopsis* root

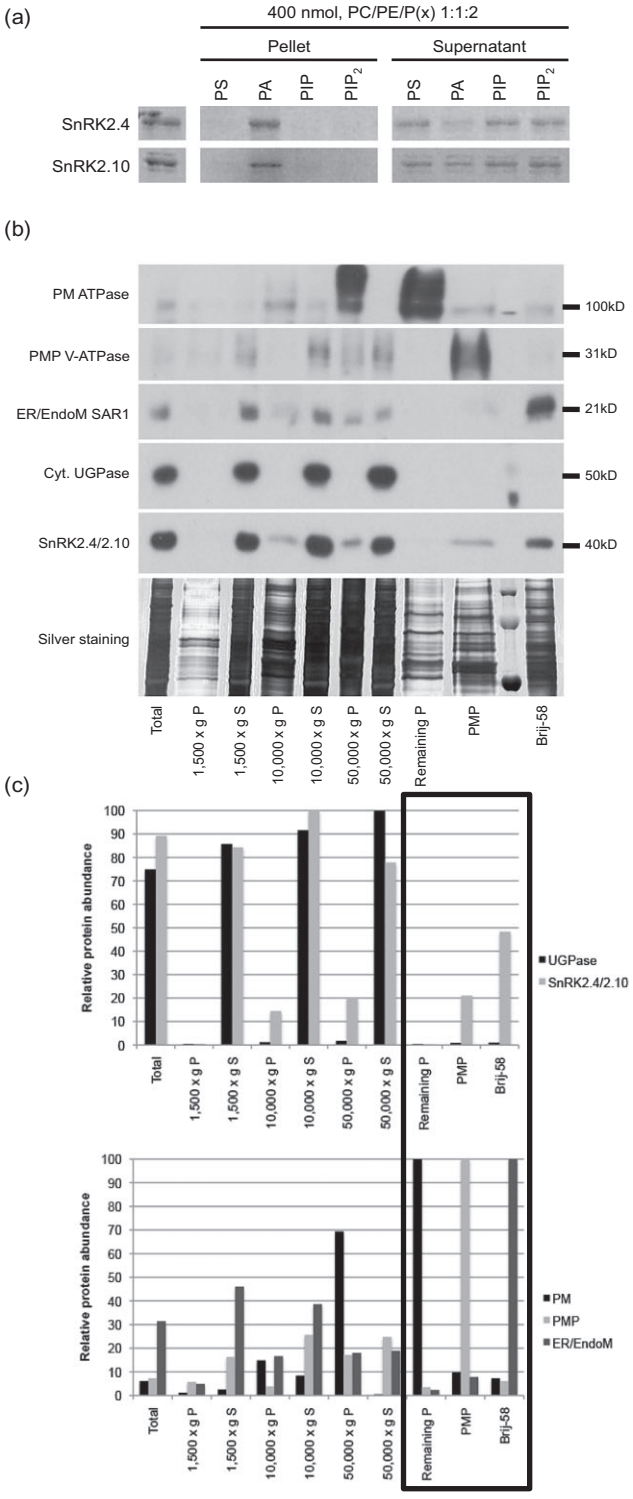


**Figure 1.** SnRK2.4 and 2.10 membrane interaction. (a) SnRK2.4 and SnRK2.10 bind specifically to the liposomes containing phosphatidic acid. GST-tagged SnRK2.4 and SnRK2.10 were incubated with 400 nmol liposomes composed of PC/PE/Px lipids in 1:1:2 ratio, where Px represents one of the anionic lipids [phosphatidylserine (PS), phosphatidic acid (PA), phosphatidylinositol-4-phosphate (PI4P) or phosphatidylinositol-4,5-biphosphate ($PIP_2$)]. The pellet fraction represents liposome-bound protein, and the supernatant fraction the unbound protein. In the left panel, the input protein is shown as a loading control. (b) SnRK2.4/2.10 is associated with the membrane after exposure to salt in *Arabidopsis* roots. Proteins from *Arabidopsis* roots treated with 150 mM NaCl for 7 min were isolated and fractionated using sequential centrifugation steps. Western blot analysis was performed on these fractions using antibodies against different compartment markers and SnRK2.4/2.10. Membranes were isolated and washed with Brij-58 to release any soluble immobilized proteins. From the upper to lower panel: Plasma membrane (PM ATPase), peripheral vacuolar membrane (PerM V-ATPase), endoplasmic reticulum and involved in trafficking between the ER and the Golgi (ER/EndoM SAR1), cytosol (UGP-ase) and SnRK2.4/2.10. In the lowest panel, a silver stain is shown as a loading control. (c) Protein quantification of the cytosolic UGPase and SnRK2.4/2.10 (upper graph) and several cellular protein markers (lower graph). The protein abundances were normalized to the highest value measured for each protein.

extracts were subjected to differential centrifugation (Fig. 1b,c). The distribution of SnRK2.4/2.10 over the different fractions is largely similar to the cytosolic marker – UDP-glucose pyrophosphorylase (UGPase), indicating that most of the SnRK2.4/2.10 is cytosolic. In addition, SnRK2.4/2.10 are also present in the 10 000 g (debris, intact organelles) and 50 000 g pellet (microsomal membranes), showing that a subpool is associated with the membrane or enclosed in cellular compartments. The 50 000 g pellet fraction was first washed with Brij-58 to release any soluble proteins trapped in cellular compartments. The Secretion-Associated and Ras-related protein1 (SAR1) involved in intracellular protein transport between the endoplasmic reticulum (ER) and the Golgi is mainly present in the ER (Pimpl *et al*. 2000). This ER marker, as well as SnRK2.4/2.10, is present in the Brij-58 wash fraction, indicating inclusion of SnRK2.4/2.10 in intracellular membrane structures, consistent with the localization into punctate structures in response to salt stress (McLoughlin *et al*. 2012). However, in contrast to the ER marker, SnRK2.4/2.10 is also present in pellet fraction obtained after Brij-58 washing, which contains the peripheral membrane protein V-ATPase epsilon subunit (At4g11150). These results show that SnRK2.4/2.10 were not just trapped in vesicular or organellar structures but were also in part directly associated with the membrane.

## Multiple regions of SnRK2.4 bind PA-containing liposomes

To narrow down the candidate region(s) that bind PA, binding affinity was first tested using liposome dilution series of the SnRK2.4 isoform (Fig. 2a). SnRK2.4 was able to bind liposomes containing 50% PA at both 400 and 40 nmol total lipid content, in contrast to the SnRK2.6 isoform, which did not bind to any of the liposomes tested. As SnRK2.6 does not exhibit any PA-binding affinity, but has high homology to other SnRK2 members that do have PA-binding affinity, protein sequences were aligned to identify amino acids that are likely to be important for PA binding. Lysine and arginine residues are known to be preferred docking sites for PA (Testerink & Munnik 2005; Kooijman *et al*. 2007). Therefore, all of the basic residues conserved in the PA-binding SnRK2s, but absent in SnRK2.6, were considered as candidate residues involved in PA binding (underlined in Fig. 2b and highlighted in red in Fig. S3).

Two candidate amino acids were found in the N-terminal kinase domain, five were identified in domain 1, which is a 42 amino acid domain that is required for the osmotic stress response, and two were found in the C-terminal acidic domain (domain 2) (Kulik *et al*. 2011). A schematic overview of SnRK2.4 domains and location of candidate amino acids is displayed in Fig. 3a. To further investigate which part of the protein contains the PABD, six fragments (A–F) of SnRK2.4 were expressed as fusion proteins in *E. coli* and purified, with an emphasis on domain 1 (fragments B, C, E and F). Fragment A consisted of the kinase domain of SnRK2.4, fragment B is the regulatory domain, fragment C covered the osmotic response domain (domain 1) and fragment D covered the

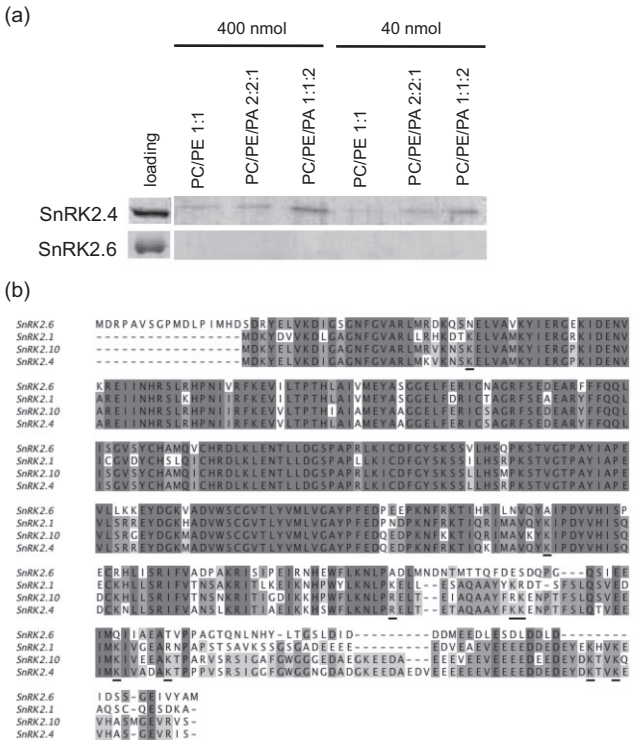


**Figure 2.** SnRK2.6 does not bind to liposomes containing phosphatidic acid (PA). (a) GST-tagged SnRK2.4 and 2.6 were expressed in *Escherichia coli* and purified. Both proteins were incubated with 400 and 40 nmol liposomes containing PC/PE/PA in the ratios 2:2:1 or 1:1:2. Pellet fractions, representing bound protein, were loaded on sodium dodecyl sulphate–polyacrylamide gel electrophoresis (SDS-PAGE) and protein was detected with anti-GST Western blot analysis. In the left panel, the input protein is shown as a loading control. (b) Amino acid sequence alignment of three SnRK2s that exhibit PA-binding affinity (SnRK2.1, 2.4 and 2.10) and SnRK2.6, which does not bind PA. Alignment was performed in Jalview using MUSCLE alignment algorithm. The percentage of sequence identity is represented by different shades of grey. Basic amino acids conserved in the SnRK2 members that have PA-binding affinity and which are absent in SnRK2.6 are underlined.

acidic domain (domain 2). As most candidate amino acids were identified in domain 1, two sub-fragments were produced for this domain; fragment E covers the N-terminal and F the C-terminal part, including the region between domains 1 and 2.

Using liposomes containing 400 nmol lipids, all indicated fragments except fragment D (domain 2) were shown to bind PA (Fig. 3b). This indicates that multiple parts of the protein could contribute to the interaction of SnRK2.4 with PA. The SnRK2.4 kinase domain has weak PA-binding affinity compared with the other fragments as it only binds to the highest concentration of liposomes tested (400 nmol). Interestingly, although the kinase domains of SnRK2.4 and 2.6 are very similar, the SnRK2.6 kinase domain, likewise SnRK2.6 full-length protein (Fig. 2a), did not show any binding affinity to liposomes containing PA (Fig. 3c). On the contrary, fragments B and C were able to bind PA even at the lowest lipid

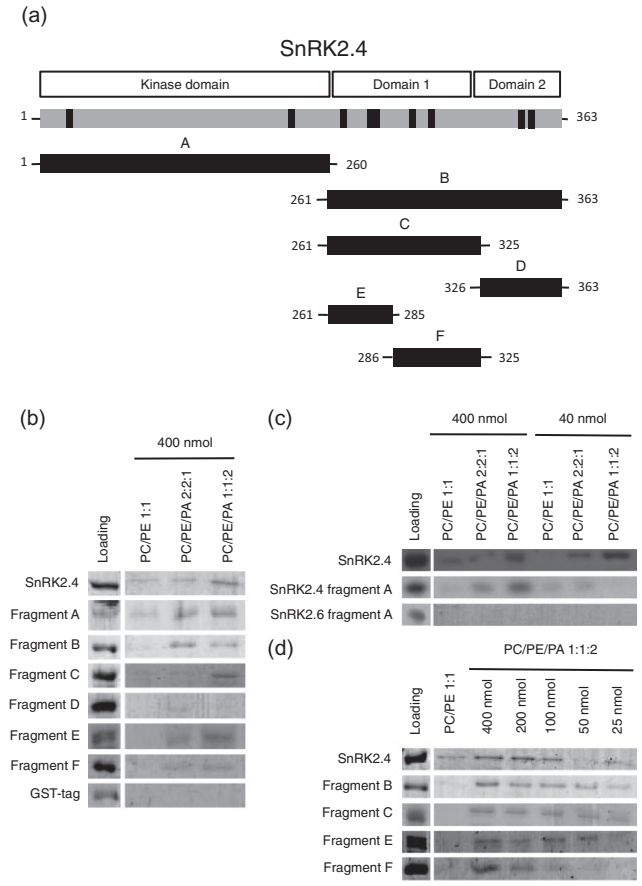


**Figure 3.** Phosphatidic acid (PA) binding occurs largely through the domain required for stress responses. (a) Schematic overview of the coding region of SnRK2.4 with several domains and the locations of the candidate amino acids highlighted in black. Below, the locations of the SnRK2.4 fragments used are displayed. (b) Kinase domain and domain 1 exhibit PA-binding affinity. GST-tagged SnRK2.4 and the fragments were expressed in *Escherichia coli* and purified. SnRK2.4, the fragments and free GST were incubated with 400 nmol of liposomes containing either PC/PE in the ratio 1:1 or PC/PE/PA in the ratios 2:2:1 or 1:1:2. (c) The kinase domain of SnRK2.6 does not bind PA. Liposome assays were conducted on full-length SnRK2.4 and the kinase domains of SnRK2.4 and 2.6 with 400 or 40 nmol liposomes containing either PC/PE in the ratio 1:1 or PC/PE/PA in the ratios 2:2:1 or 1:1:2. (d) Differences in PA-binding affinity of different truncated SnRK2.4 fragments. SnRK2.4 and a selection of truncated fragments were incubated with different amounts of liposomes ranging between 400 and 25 nmol containing either PC/PE 1:1 or PC/PE/PA 1:1:2. Pellet fractions, representing bound protein, were loaded on sodium dodecyl sulphate–polyacrylamide gel electrophoresis (SDS-PAGE) and protein was detected with anti-GST Western analysis. In the left panels, the input protein is shown as a loading control.

concentration tested (25 nmol). This indicates that the fragments containing the abiotic stress domain 1 have the highest PA-binding affinity. The PA-binding strength of fragment E and fragment F were both lower than that of the B and C fragments, suggesting that PA binding was located C-terminally in domain 1, known to be required for ABA-independent activation in the response to osmotic stress (Kulik *et al*. 2011).

## Basic amino acids present in domain 1 are necessary for PA binding

A new fragment corresponding to domain 1, which encompasses the E fragment and the N-terminal part of fragment F (261–302), was expressed as a fusion protein and showed similar (or even higher) affinity for PA as the full-length protein (Fig. 4a). Within this PABD, the five candidate basic amino acids (fragment C; Fig. 3a) were mutated to alanines. The resulting PABD mutant PABD$^{R266A,\ K278A,\ K279A,\ K294A,\ K300A}$ did not exhibit any PA-binding affinity (Fig. 4a), showing that these amino acids are indeed essential for PA-binding capacity of the domain. The significance of the five candidate amino acids present in the PABD was subsequently examined in the context of the full-length SnRK2.4 protein. A SnRK2.4$^{R266A,\ K278A,\ K279A,\ K294A,\ K300A}$ mutant protein exhibited similar or only slightly reduced PA-binding affinity at all lipid concentrations tested (Supporting Information Fig. S1). As the kinase domain also exhibited some PA-binding affinity (fragment A; Fig. 3b), the candidate amino acids in the kinase domain were additionally mutated in the full-length protein. Surprisingly, the SnRK2.4$^{K27A,\ K222A,\ R266A,\ K278A,\ K279A,\ K294A,\ K300A}$ still retained PA-binding capacity (Supporting Information Fig. S1). Summarizing, our *in vitro* lipid binding data indicate that although basic amino acid-based PA-binding of domain 1 represents the highest PA-binding affinity site within SnRK2.4, additional residues contribute to the lipid binding affinity of the full-length SnRK2.4 protein.

## SnRK2.4 re-localization into punctate structures does not solely depend upon the identified PABD

SnRK2.4 re-localized to punctate structures in response to salt stress (McLoughlin *et al*. 2012) in which PA binding might play a role. In order to determine the contribution of the SnRK2.4 PABD to the re-localization, the PABD was fused to YFP and expressed in *Arabidopsis* under control of the ubiquitin promoter (UBQ). Unlike SnRK2.4-YFP (Fig. 4c), the PABD-YFP fusion did not accumulate in punctate structures during salt stress in root epidermal cells in several independent transgenic lines (Fig. 4e). These results indicate that SnRK2.4 re-localization does not rely solely upon the PA–PABD interaction. The mechanism of SnRK2.4 re-localization might depend on coincidence detection, where other domains are required to open up the structure exposing PABD for its interaction with PA. Further, additional protein–protein interactions might be necessary before SnRK2.4 can be incorporated in the punctate structures.

SnRK2.10, which also binds to PA, and which is highly similar in protein sequence to SnRK2.4 (Fig. 1), was previously observed to remain in the cytosol in saline conditions (McLoughlin *et al*. 2012). This could be explained since SnRK2.10 is expressed in different root tissues and no expression was observed in cell types where SnRK2.4 re-localization was observed. Therefore, the lack of re-localization of SnRK2.10 in response to salt could be due to cell-specific PA-increase in epidermis rather than a

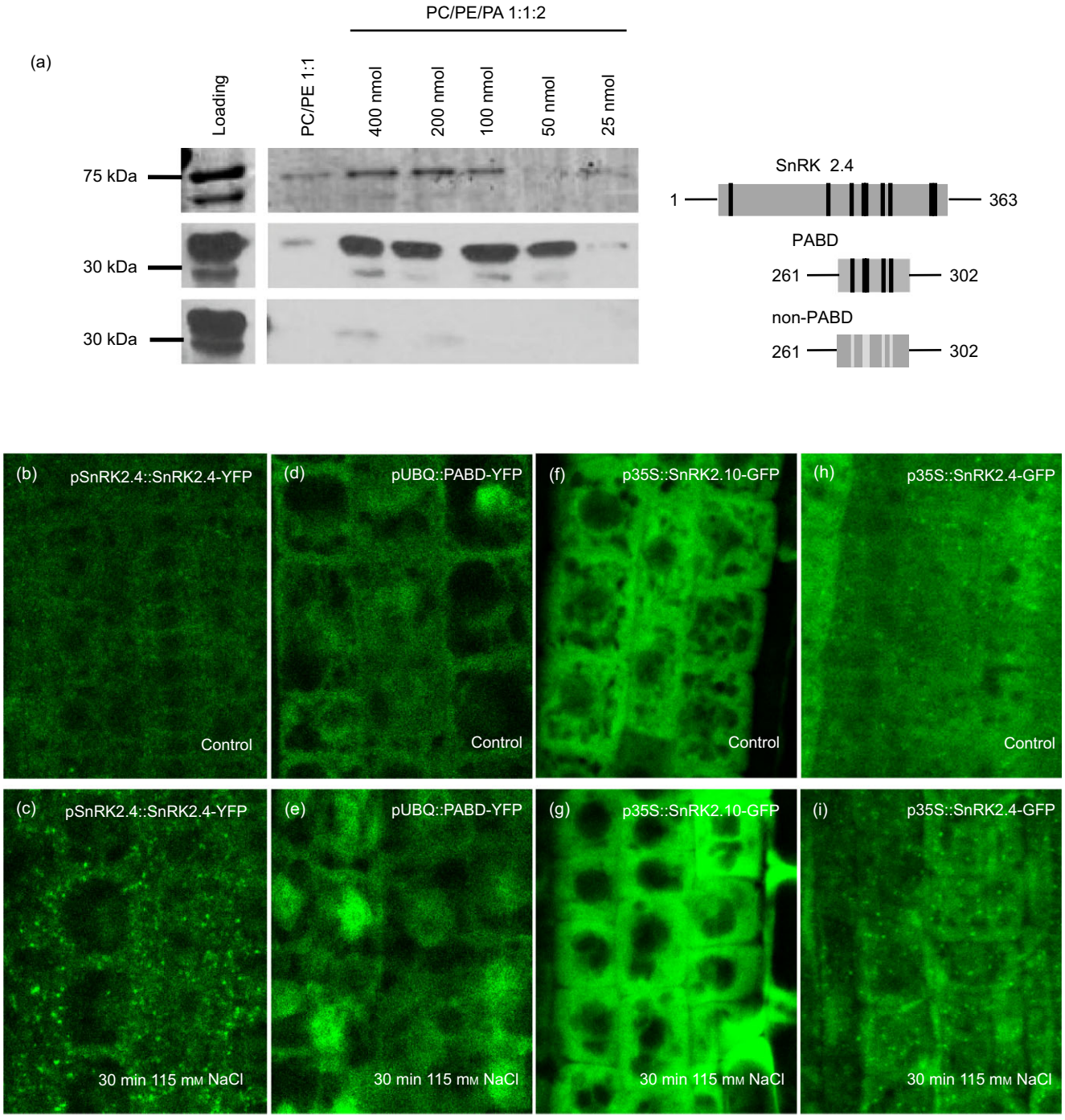


**Figure 4.** Phosphatidic acid (PA) binding of the PA-binding domain relies upon conserved basic amino acids, but is not sufficient for salt-induced re-localization. (a) Conserved basic amino acids in the PA-binding domain are prerequisite for PA binding of this domain. GST-tagged SnRK2.4, PA-binding domain and non-PABD$^{R266A, K278A, K279A, K294A, K300A}$, where five conserved basic amino acids were mutated to alanine, were expressed in *Escherichia coli* and purified. GST protein fusions were incubated with different amounts of liposomes ranging between 400 and 25 nmol containing either PC/PE 1:1 or PC/PE/PA 1:1:2. The loading control is shown in the left panels and the proteins that bound to the liposomes are shown in the middle panels. A schematic representation of the SnRK2.4, PA-binding domain with the selected lysines and arginines (black) and the same amino acids mutated to alanine (light grey) in non-PABD are represented in the right panels. (b) Binding to PA is not sufficient for re-localization into punctate structures. While full-length SnRK2.4-YFP protein fusion is changing its cytosolic localization in root epidermis cells in control conditions to (c) punctate structures after salt stress treatment, (d) PABD-YFP protein fusion was observed to localize in cytosol under control and (e) salt stress conditions in root epidermis cells (f) SnRK2.10-GFP protein fusion localization in root epidermis cells was studied using SnRK2.10-GFP overexpression line. SnRK2.10-GFP localized at cytosol in control and (g) salt stress conditions, (h) overexpression of SnRK2.4-GFP line was used as a positive control. SnRK2.4-GFP localized at cytosol in control conditions but (i) significant fraction re-localized into punctate structures upon salt stress treatment.

difference in protein sequence. To test this hypothesis, localization of SnRK2.10 in epidermal cells was examined in stably transformed lines expressing the protein under control of the 35S promoter. The cellular localization of p35S::SnRK2.10-GFP protein expressed in epidermal cell layers was found to be restricted to the cytosol, in control as well as in salt stress conditions (Fig. 4f,g), whereas p35S::SnRK2.4-GFP fusion protein was observed to re-localize into punctate structures after exposure to salt stress (Fig. 4h,i). This suggests that differences in protein sequence between SnRK2.10 and SnRK2.4 rather than their tissue-specific expression are responsible for the difference in re-localization into punctate structures, again indicating that besides the conserved PABD, other domains within these proteins are relevant for the re-localization.

## Overexpression of a functional SnRK2.4 PABD leads to root growth reduction

The PABD of SnRK2.4 protein overlaps with domain 1, which is conserved in all SnRK2 isoforms, and needed for activation upon abiotic stress, independently of ABA (Kulik *et al*. 2011). The function of this domain 1 is largely unknown. In order to investigate the effect of the PABD/domain 1 on seedling growth, the *wt* PABD (UBQ::PABD-YFP) as well as the non-PA-binding mutant version $PABD^{R266A,\ K278A,\ K279A,\ K294A,\ K300A}$ (UBQ::non-PABD-mCherry) were expressed in *Arabidopsis* (Supporting Information Fig. S4). Overexpression of the PABD-YFP was found to significantly reduce main root length, lateral root density and total root size as well as rosette size of 8-day-old seedlings grown on agar plates, whereas no reduction in seedling growth was observed in lines overexpressing the non-PABD (Fig. 5). These results show that domain 1 of SnRK2.4 has a negative impact on seedling root growth and also highlight a role for PA binding of this domain in the observed phenotype.

## DISCUSSION

The SnRK2.4 and SnRK2.10 protein kinases are rapidly activated by salt stress (McLoughlin *et al*. 2012) in an ABA-independent manner (Boudsocq *et al*. 2007). SnRK2.4 and SnRK2.10 were initially identified in a screen for PA-binding proteins (Testerink *et al*. 2004) and were functionally characterized to have a role in root growth in saline conditions (McLoughlin *et al*. 2012). This study focuses on the characterization of the PABD of SnRK2.4 and SnRK2.10 and the significance of this interaction for SnRK2.4 function *in planta*.

The observed specificity of SnRK2.4 and 2.10 for binding PA (Fig. 1a) indicates the presence of a specific PA-binding site, rather than a general, electrostatic interaction with anionic lipids. As both PIP and PIP2 have significantly more charge than PA (Kooijman & Burger 2009) and even 50% anionic lipid did not induce binding to membranes containing PS, PIP and PIP2, our data suggest that SnRK2.4 and 2.10 membrane binding is truly specific for PA. Comparing the presence of SnRK2.4/2.10 in endosomal membrane fractions to V-ATPase and SAR1 revealed that a small fraction of SnRK2.4/2.10 was associated with membranes (Fig. 1b). A major fraction of the SnRK2.4/2.10 present in the microsomal membrane fraction was released during the Brij-58 wash (together with the SAR1 marker), showing that the majority of SnRK2.4/2.10 proteins are contained in the vesicles rather than bound to the lipid bilayer.

By testing different SnRK2.4 protein fragments for PA binding, multiple PA-binding sites were identified. The strongest PA-binding affinity was found for domain 1 in the C-terminal domain of the protein, and weaker affinity for the kinase domain. The presence of multiple lipid binding domains present in a protein has been observed before, in yeast Opi1 protein (Loewen *et al*. 2004), as well as in plant TGD4 (Wang *et al*. 2013). The final binding strength and specificity of SnRK2.4 to certain PA pools may be dependent upon allosteric mechanisms, exposing different PABDs within the SnRK2.4 protein structure. PA preferentially interacts with lysines and arginines (Testerink & Munnik 2005; Kooijman *et al*. 2007), and site-directed mutagenesis of basic amino acids has shown to be effective in abolishing PA binding of several PA targets (Ghosh *et al*. 2003; Zhang *et al*. 2004, 2009; Wang *et al*. 2006). Five positively charged amino acid residues (lysines and arginines), conserved in the PABD (domain 1) of the class 1 SnRK2 members, were identified as possible PA-binding residues. Indeed, mutation of these candidate amino acids completely abolished PA-binding affinity of the SnRK2.4 PABD (Fig. 4a). In the context of the full-length protein, however, mutating these five residues to alanine did not reduce the PA-binding affinity *in vitro* over a range of different lipid concentrations (Supporting Information Fig. S1). Surprisingly, mutation of additional amino acids in the kinase domain did not disrupt the binding affinity either (Supporting Information Fig. S1). These results suggest the existence of more domains that enable PA binding, but are distinct from conserved basic residues present in the kinase domain and the PABD/domain 1.

Binding to PA through the PABD alone is not sufficient for salt-induced re-localization, as the PABD remained in the cytosol after salt stress exposure (Fig. 4e). The re-localization into the punctate structures apparently requires additional SnRK2.4 protein–protein or protein–membrane interactions through other regions of the full-length protein. This conclusion is supported by studies that use a SnRK2.10 overexpression line. The homology between SnRK2.4 and 2.10 is high (89% protein sequence identity) and both protein kinases bind PA *in vitro* (Fig. 1a) (McLoughlin *et al*. 2012). Yet re-localization into punctate structures was not observed in the line overexpressing SnRK2.10-GFP (Fig. 4g). Together, this suggests that re-localization is not only dependent upon conserved basic amino acids present in the PABD of both SnRK2s but also involves additional mechanisms that remain to be identified. These mechanisms could rely upon coincidence detection of lipids, requiring multiple PA-binding sites that do differ in the protein sequences of SnRK2.4 and SnRK2.10 (Supporting Information Fig. S2), but could also be due to post-translational modifications or interactions with other proteins.

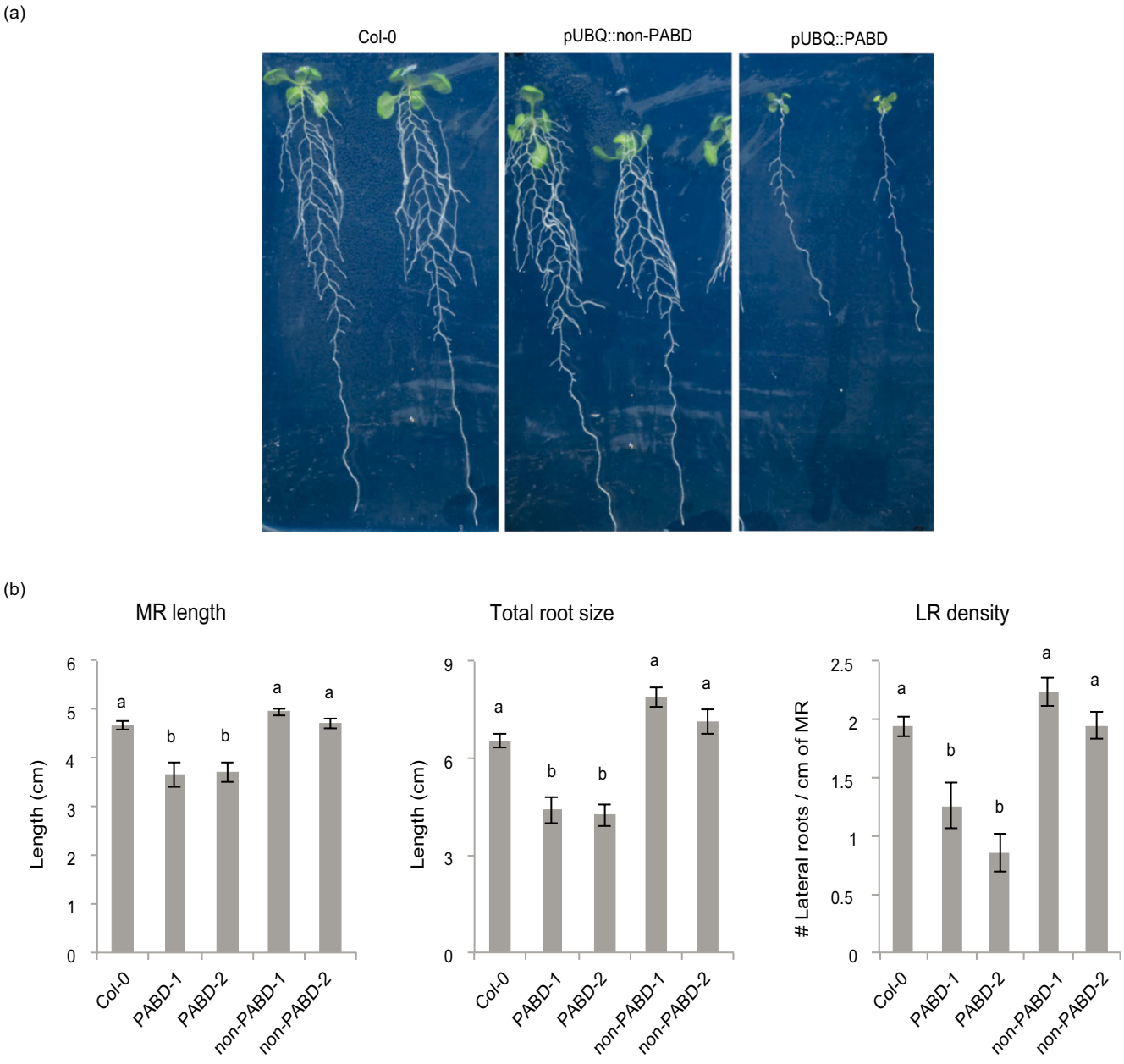


**Figure 5.** Overexposure of phosphatidic acid-binding domain PABD results in root growth reduction. Effect of PABD on root system architecture was estimated by growing seedlings of Col-0, pUBQ::PABD$^{R266A,\ K278A,\ K279A,\ K294A,\ K300A}$::RFP (pUBQ::non-PABD) and pUBQ::PABD::YFP (pUBQ::PABD) lines on agar plates: (a) root system architecture of 12-day-old seedlings and (b) root system architecture of 8-day-old seedlings grown in control conditions was quantified using EZ-Rhizo software. The bars represent the average values. $n = 16$. Error bars represent SE. Significance levels were calculated using Scheffe post-hoc test – different letters represent groups with significance < 0.05.

Overexpression of the identified SnRK2.4 PABD was found to affect *Arabidopsis* growth by reducing shoot size and root length (Fig. 5). Interestingly, the overexpression of a non-PABD (PABD$^{R266A,\ K278A,\ K279A,\ K294A,\ K300A}$) did not affect seedling growth. The observed reduction in root growth could be due to impairing normal SnRK2.4 function independently of PA, through competition for proteins or elements that interact with domain 1. Domain 1 is conserved in all class 1 SnRK2 members (Supporting Information Fig. S3) and is required for activation by osmotic stress (Kulik *et al*. 2011). Alternatively, many PA targets have been described to be important for root development and acclimation in adverse conditions (McLoughlin & Testerink 2013). Overexpression of a PABD might reduce PA available for interaction with other proteins and could therefore disrupt the functionality of several of these proteins, resulting in growth defects. In either case, it clearly shows that SnRK2.4 PABD/domain 1 plays a role in root growth, which deserves further investigation.

## ACKNOWLEDGMENTS

We thank Grazyna Dobrowolska (Polish Academy of Sciences) for advice on SnRK2 protein analysis, Xavier Zarza for technical help, and the Van Leeuwenhoek Centre for Advanced Microscopy (LCAM) at the University of Amsterdam for making their confocal microscopes available and for technical support. This work was supported by the Netherlands Organisation for Scientific Research (NWO) (Grants Vidi 700.56.429, ALW 820.02.017 and ALW 846.11.002), STW Learning from Nature (10987), NGI Horizon (project 93511011) and the U.S. National Science Foundation I2CAM International Materials Institute Award (Grant DMR-0844115).

## REFERENCES

Arisz S.A., Testerink C. & Munnik T. (2009) Plant PA signaling via diacylglycerol kinase. *Biochimica et Biophysica Acta* **1791,** 869–875.

Arisz S.A., van Wijk R., Roels W., Zhu J.K., Haring M.A. & Munnik T. (2013) Rapid phosphatidic acid accumulation in response to low temperature stress in Arabidopsis is generated through diacylglycerol kinase. *Frontiers in Plant Science* **4,** 1.

Armengaud P. (2009) EZ-Rhizo software: the gateway to root architecture analysis. *Plant Signaling & Behavior* **4,** 139–141.

Bargmann B.O. & Munnik T. (2006) The role of phospholipase D in plant stress responses. *Current Opinion in Plant Biology* **9,** 515–522.

Bargmann B.O., Laxalt A.M., ter Riet B., van Schooten B., Merquiol E., Testerink C., . . . Munnik T. (2009) Multiple PLDs required for high salinity and water deficit tolerance in plants. *Plant and Cell Physiology* **50,** 78–89.

Boudsocq M. & Lauriere C. (2005) Osmotic signaling in plants: multiple pathways mediated by emerging kinase families. *Plant Physiology* **138,** 1185–1194.

Boudsocq M., Barbier-Brygoo H. & Lauriere C. (2004) Identification of nine sucrose nonfermenting 1-related protein kinases 2 activated by hyperosmotic and saline stresses in *Arabidopsis thaliana*. *The Journal of Biological Chemistry* **279,** 41758–41766.

Boudsocq M., Droillard M.J., Barbier-Brygoo H. & Lauriere C. (2007) Different phosphorylation mechanisms are involved in the activation of sucrose non-fermenting 1 related protein kinases 2 by osmotic stresses and abscisic acid. *Plant Molecular Biology* **63,** 491–503.

Clough S.J. & Bent A.F. (1998) Floral dip: a simplified method for Agrobacterium-mediated transformation of *Arabidopsis thaliana*. *The Plant Journal* **16,** 735–743.

Dhonukshe P., Huang F., Galvan-Ampudia C.S., Mahonen A.P., Kleine-Vehn J., Xu J., . . . Offringa R. (2010) Plasma membrane-bound AGC3 kinases phosphorylate PIN auxin carriers at TPRXS(N/S) motifs to direct apical PIN recycling. *Development (Cambridge, England)* **137,** 3245–3255.

Djafi N., Vergnolle C., Cantrel C., Wietrzynski W., Delage E., Cochet F., . . . Ruelland E. (2013) The Arabidopsis DREB2 genetic pathway is constitutively repressed by basal phosphoinositide-dependent phospholipase C coupled to diacylglycerol kinase. *Frontiers in Plant Science* **4,** 307.

Fujii H., Chinnusamy V., Rodrigues A., Rubio S., Antoni R., Park S.Y., . . . Zhu J.K. (2009) *In vitro* reconstitution of an abscisic acid signalling pathway. *Nature* **462,** 660–664.

Galinha C., Hofhuis H., Luijten M., Willemsen V., Blilou I., Heidstra R. & Scheres B. (2007) PLETHORA proteins as dose-dependent master regulators of Arabidopsis root development. *Nature* **449,** 1053–1057.

Ghosh S., Moore S., Bell R.M. & Dush M. (2003) Functional analysis of a phosphatidic acid binding domain in human Raf-1 kinase: mutations in the phosphatidate binding domain lead to tail and trunk abnormalities in developing zebrafish embryos. *The Journal of Biological Chemistry* **278,** 45690–45696.

Gomez-Merino F.C., Arana-Ceballos F.A., Trejo-Tellez L.I., Skirycz A., Brearley C.A., Dormann P. & Mueller-Roeber B. (2005) Arabidopsis AtDGK7, the smallest member of plant diacylglycerol kinases (DGKs), displays unique biochemical features and saturates at low substrate concentration: the DGK inhibitor R59022 differentially affects AtDGK2 and AtDGK7 activity in vitro and alters plant growth and development. *The Journal of Biological Chemistry* **280,** 34888–34899.

Hong Y., Pan X., Welti R. & Wang X. (2008) Phospholipase Dalpha3 is involved in the hyperosmotic response in Arabidopsis. *The Plant Cell* **20,** 803–816.

Julkowska M.M., Rankenberg J.M. & Testerink C. (2013) Liposome-binding assays to assess specificity and affinity of phospholipid-protein interactions. *Methods in Molecular Biology* **1009,** 261–271.

Kobayashi Y., Yamamoto S., Minami H., Kagaya Y. & Hattori T. (2004) Differential activation of the rice sucrose nonfermenting1-related protein kinase2 family by hyperosmotic stress and abscisic acid. *The Plant Cell* **16,** 1163–1177.

Kooijman E.E. & Burger K.N. (2009) Biophysics and function of phosphatidic acid: a molecular perspective. *Biochimica et Biophysica Acta* **1791,** 881–888.

Kooijman E.E., Tieleman D.P., Testerink C., Munnik T., Rijkers D.T., Burger K.N. & de Kruijff B. (2007) An electrostatic/hydrogen bond switch as the basis for the specific interaction of phosphatidic acid with proteins. *The Journal of Biological Chemistry* **282,** 11356–11364.

Kulik A., Wawer I., Krzywinska E., Bucholc M. & Dobrowolska G. (2011) SnRK2 protein kinases – key regulators of plant response to abiotic stresses. *Omics: A Journal of Integrative Biology* **15,** 859–872.

Loewen C.J., Gaspar M.L., Jesch S.A., Delon C., Ktistakis N.T., Henry S.A. & Levine T.P. (2004) Phospholipid metabolism regulated by a transcription factor sensing phosphatidic acid. *Science* **304,** 1644–1647.

McLoughlin F. & Testerink C. (2013) Phosphatidic acid, a versatile water-stress signal in roots. *Frontiers in Plant Science* **4,** 525.

McLoughlin F., Galvan-Ampudia C.S., Julkowska M.M., Caarls L., van der Does D., Lauriere C., . . . Testerink C. (2012) The Snf1-related protein kinases SnRK2.4 and SnRK2.10 are involved in maintenance of root system architecture during salt stress. *The Plant Journal* **72,** 436–449.

McLoughlin F., Arisz S.A., Dekker H.L., Kramer G., de Koster C.G., Haring M.A., . . . Testerink C. (2013) Identification of novel candidate phosphatidic acid-binding proteins involved in the salt-stress response of *Arabidopsis thaliana* roots. *The Biochemical Journal* **450,** 573–581.

Meijer H.J. & Munnik T. (2003) Phospholipid-based signaling in plants. *Annual Review of Plant Biology* **54,** 265–306.

Mikolajczyk M., Awotunde O.S., Muszynska G., Klessig D.F. & Dobrowolska G. (2000) Osmotic stress induces rapid activation of a salicylic acid-induced protein kinase and a homolog of protein kinase ASK1 in tobacco cells. *The Plant Cell* **12,** 165–178.

Mizoguchi M., Umezawa T., Nakashima K., Kidokoro S., Takasaki H., Fujita Y., . . . Shinozaki K. (2010) Two closely related subclass II SnRK2 protein kinases cooperatively regulate drought-inducible gene expression. *Plant and Cell Physiology* **51,** 842–847.

Monreal J.A., McLoughlin F., Echevarria C., Garcia-Maurino S. & Testerink C. (2010) Phosphoenolpyruvate carboxylase from C4 leaves is selectively targeted for inhibition by anionic phospholipids. *Plant Physiology* **152,** 634–638.

Munnik T. & Vermeer J.E. (2010) Osmotic stress-induced phosphoinositide and inositol phosphate signalling in plants. *Plant, Cell & Environment* **33,** 655–669.

Munnik T., Ligterink W., Meskiene I.I., Calderini O., Beyerly J., Musgrave A. & Hirt H. (1999) Distinct osmo-sensing protein kinase pathways are involved in signalling moderate and severe hyper-osmotic stress. *The Plant Journal* **20,** 381–388.

Nagai T., Ibata K., Park E.S., Kubota M., Mikoshiba K. & Miyawaki A. (2002) A variant of yellow fluorescent protein with fast and efficient maturation for cell-biological applications. *Nature Biotechnology* **20,** 87–90.

Palmgren M.G., Sommarin M., Serrano R. & Larsson C. (1991) Identification of an autoinhibitory domain in the C-terminal region of the plant plasma membrane H(+)-ATPase. *The Journal of Biological Chemistry* **266,** 20470–20475.

Pierik R. & Testerink C. (2014) The art of being flexible: how to escape from shade, salt and drought. *Plant Physiology*. doi: http://dx.doi.org/10.1104/pp.114.239160.

Pimpl P., Movafeghi A., Coughlan S., Denecke J., Hillmer S. & Robinson D.G. (2000) *In situ* localization and in vitro induction of plant COPI-coated vesicles. *The Plant Cell* **12,** 2219–2236.

Testerink C. & Munnik T. (2005) Phosphatidic acid: a multifunctional stress signaling lipid in plants. *Trends in Plant Science* **10,** 368–375.

Testerink C. & Munnik T. (2011) Molecular, cellular, and physiological responses to phosphatidic acid formation in plants. *Journal of Experimental Botany* **62,** 2349–2361.

Testerink C., Dekker H.L., Lim Z.Y., Johns M.K., Holmes A.B., Koster C.G., . . . Munnik T. (2004) Isolation and identification of phosphatidic acid targets from plants. *The Plant Journal* **39,** 527–536.

Umezawa T., Yoshida R., Maruyama K., Yamaguchi-Shinozaki K. & Shinozaki K. (2004) SRK2C, a SNF1-related protein kinase 2, improves drought tolerance by controlling stress-responsive gene expression in *Arabidopsis thaliana*. *Proceedings of the National Academy of Sciences of the United States of America* **101,** 17306–17311.

Vlad F., Droillard M.J., Valot B., Khafif M., Rodrigues A., Brault M., . . . Lauriere C. (2010) Phospho-site mapping, genetic and in planta activation studies reveal key aspects of the different phosphorylation mechanisms involved in activation of SnRK2s. *The Plant Journal* **63,** 778–790.

Wang X. (2004) Lipid signaling. *Current Opinion in Plant Biology* **7,** 329–336.

Wang X., Devaiah S.P., Zhang W. & Welti R. (2006) Signaling functions of phosphatidic acid. *Progress in Lipid Research* **45,** 250–278.

Wang Z., Anderson N.S. & Benning C. (2013) The phosphatidic acid binding site of the Arabidopsis trigalactosyldiacylglycerol 4 (TGD4) protein required for lipid import into chloroplasts. *The Journal of Biological Chemistry* **288,** 4763–4771.

Xue H.W., Chen X. & Mei Y. (2009) Function and regulation of phospholipid signalling in plants. *The Biochemical Journal* **421,** 145–156.

Zhang W., Qin C., Zhao J. & Wang X. (2004) Phospholipase D alpha 1-derived phosphatidic acid interacts with ABI1 phosphatase 2C and regulates abscisic acid signaling. *Proceedings of the National Academy of Sciences of the United States of America* **101,** 9508–9513.

Zhang Y., Zhu H., Zhang Q., Li M., Yan M., Wang R., . . . Wang X. (2009) Phospholipase dalpha1 and phosphatidic acid regulate NADPH oxidase activity and production of reactive oxygen species in ABA-mediated stomatal closure in Arabidopsis. *The Plant Cell* **21,** 2357–2377.

*Received 15 April 2014; received in revised form 17 July 2014; accepted for publication 20 July 2014*

## SUPPORTING INFORMATION

Additional Supporting Information may be found in the online version of this article at the publisher's web-site:

**Figure S1.** PA-binding in full length SnRK2.4 protein context is not abolished by mutations of conserved basic amino acids.

**Figure S2.** Alignment between SnRK2.4 and SnRK2.10 protein sequence.

**Figure S3.** Alignment of protein sequences of all SnRK2 family members.

**Figure S4.** Identification of fusion proteins with YFP/mCherry.

**Table S1.** Primer sequences.